

Confined boiling of FC72 and FC87 on a downward facing heating copper disk

J.C. Passos^{a,*}, F.R. Hirata^a, L.F.B. Possamai^a, M. Balsamo^b, M. Misale^b

^a Departamento de Engenharia Mecânica, LABSOLAR-NCTS, Universidade Federal de Santa Catarina, Cx. P. 476, 88010-900 Florianópolis, S.C., Brazil

^b Dipartimento di Termoeconomica e Condizionamento Ambientale, Via All'Opera Pia, 15-a, (I) 16145 Genova, Italy

Abstract

This paper presents results for FC72 and FC87 saturated and subcooled nucleate pool boiling, at atmospheric pressure, on a downward facing surface and in confined spaces between a heated copper disk (diameter 12 mm and thickness 2 mm) and an unheated surface, for distances varying between 0.2 and 13 mm. At saturated boiling and low heat flux ($\leq 45 \text{ kW/m}^2$) a decrease in the distance between the plates causes an enhancement of the boiling. At subcooled boiling the results show that the heat transfer coefficient decreases with a reduction in the distance between the plates. A visualization of the subcooled boiling shows the effect of confinement and heat flux on the liquid–vapor configuration.

© 2003 Elsevier Inc. All rights reserved.

Keywords: Nucleate boiling; Bond number; Confined boiling; Phase change; Heat transfer

1. Introduction

The nucleate boiling regime can present a particular behaviour when working, under low heat flux, in a confined space or on surfaces with a high inclination angle. For several geometrical configurations, the confinement level can be represented by the Bond number, Yao and Chang (1983) defined as the ratio of a characteristic dimension (s) of the confined space to the capillary length. The latter is given by the following equation:

$$L = \left[\frac{\sigma}{g(\rho_l - \rho_v)} \right]^{1/2} \quad (1)$$

where σ , g , ρ_l and ρ_v represent the surface tension, the acceleration due to gravity, the vapour density and the liquid density, respectively.

Ishibashi and Nishikawa (1969) obtained results for boiling in the narrow vertical annulus formed by a cylindrical heated bar and an unheated tube and classified two regimes: isolated bubbles and coalesced bub-

bles. Katto et al. (1977) studied the saturated water nucleate boiling in the space between two horizontal disks, one heated facing upward and the other unheated, for different distances from 0.1 to 2 mm and also for a simple heated disk in a pool. The general trend of these previous studies shows under low heat flux that the heat transfer coefficient increases as s decreases, when s is not very small. The results of Katto et al. (1977) showed a very fast decrease in the heat transfer coefficient for water when $s = 0.1$ mm, corresponding to a Bond number of 0.04. Yao and Chang (1983) presented results for R-113, water and acetone pool boiling inside vertical annuli with heights of 25.4 and 76.4 mm and gaps of 0.32, 0.80 and 2.58 mm. In addition to the Bond number these authors considered the effect of the aspect ratio of the channel and defined a modified boiling number as the ratio of the residence time of the bubble in the confined space to the vapour formation time, as reviewed in Passos et al. (2002). Geisler and Bar-Cohen (2003) analysed the nucleate boiling and critical heat flux inside vertical channels for FC72 with s values between 0.3 and 1.6 mm, and for the unconfined case they obtained a good fit between experimental data and that correlated by Rohsenow's correlation (Carey, 1992) using the coefficient $C_{sf} = 0.0055$.

* Corresponding author. Tel.: +55-48-331-9379; fax: +55-48-234-15-19.

E-mail address: jpassos@emc.ufsc.br (J.C. Passos).

Nomenclature

g	acceleration of gravity, m/s^2	ρ	density, kg/m^3
h	heat transfer coefficient, $\text{W/m}^2 \text{K}$	σ	surface tension, J/m^2
L	capillary length, m	<i>Subscripts</i>	
q	heat flux, W/m^2	l	liquid
s	distance between the heating plate and the bottom of the boiling chamber, m, mm	v	vapor
t	temperature, $^\circ\text{C}$	sat	saturation
ΔT	difference of temperature, $^\circ\text{C}$	w	wall

The increase in the heat transfer coefficient for confined boiling is explained by Katto et al. (1977) as the result of evaporation of the liquid film between the bubble and the heating wall, in the case of flattened bubbles, because with the narrow gap the surface area of the thin liquid film is increased.

The maximum heat flux, represented by the critical (CHF) or dryout (DHF) heat flux, allowing a system to operate in nucleate boiling can be highly dependent on the confinement and the general trend is its decrease with a decrease in s , as reported by Katto et al. (1977), Yao and Chang (1983), Bonjour and Lallemand (1997) and Geisler and Bar-Cohen (2003).

For systems operating at low and moderate heat flux, when compared with the critical or dryout heat flux, the orientation of the heating surface with the gravity vector can influence the mechanisms of heat transfer. Nishikawa et al. (1984) show for saturated water nucleate boiling that under low heat flux the heat transfer coefficient increases with an increase in the angle of inclination (θ), from a horizontal upward facing ($\theta = 0^\circ$) to an almost horizontal downward facing flat plate ($\theta = 175^\circ$). Nishikawa et al. (1984) explained this enhancement as an effect of the increase of the natural convection boundary layer thickness that allows the nucleation for lower superheating of the wall and an intensification in the vaporization of the liquid film between the interface of each bubble and the wall when the bubbles move along the surface escaping via the lateral edges. For high heat flux the curves for different inclinations follow a single path. Chang and You (1996) analysed the effects of surface orientation on saturated FC72 pool boiling, at atmospheric pressure, on a micro-porous-enhanced square heater (10×10 mm mounted in a support of 40×40 mm) compared with a plain copper plate. The interest in this study is related to some data concerning the enhancement of boiling for the horizontal plain plate in the downward position. Contrary to Nishikawa et al. (1984), the data presented by Chang and You (1996) are not so clear concerning the effect of the inclination on the heat transfer coefficient and this is attributed to the mode of heating, with an increase in the heat flux, whereas in the case of Nishikawa et al. (1984)

the heat flux is decreased. Arlabosse et al. (1998) visualized the flow around an air bubble on a heated brass plate in contact with silicon oil in which a temperature gradient was set up by cooling from the bottom of the chamber. This flow is called the Marangoni flow and is induced by thermocapillary action caused by the variation in surface tension with temperature (Carey, 1992).

The magnitude of the gravitational acceleration can influence the boiling mechanisms. For conditions of micro-gravity the bubbles on the heated wall are bigger compared with those for terrestrial gravity as reported by Straub et al. (1990). In the former case, the heat transfer mechanism is also due to the Marangoni flow.

The objective of this work is the experimental investigation of FC72 and FC87 in a confined space and with downward facing surface pool boiling heat transfer, for saturated and subcooled conditions. The motivation of this study is the understanding of the boiling mechanisms under the confinement conditions encountered in many of the recent two-phase flow applications such as solar energy thermosyphons and some devices used in the control of satellite applications such as heat pipes and capillary pumps. The test section used in this experiment is similar to those of a proposed experiment to be included in the French–Brazilian micro-satellite which is expected to be launched in 2005.

2. Experiment

The tests were performed in FC72 and FC87 pools, at atmospheric pressure, at LABSOLAR/NCTS of Federal University of Santa Catarina, in Brazil.

Fig. 1 shows the experimental apparatus, consisting of the boiling experiment and the data acquisition system and on the ground a cryostat to control the temperature of the water bath, in the square box. Immersed in the water bath is the boiling chamber consisting of a glass tube of 50 mm diameter containing the working fluid (FC72 or FC87) and the test section immersed in it. The tests were carried out with 0.14 liter in the boiling chamber, filled to 60–70% capacity. The test section consists of a copper disk with diameter 12 mm and



Fig. 1. Experimental apparatus.

thickness 2 mm placed centred at the end of a PVC support with diameter 20 mm placed at the end of a stainless steel tube support. The distance between the copper disk and the base of the boiling chamber is adjustable by turning the stainless steel tube and controlling the distance by means of a dial indicator, see Fig. 1 on the top of the boiling chamber. The copper disk is heated by a skin heater of 11.2Ω and is fitted in the middle with an E thermocouple of 0.15 mm diameter, immersed in the copper disk. Three other E thermocouples (TC) are immersed in the pool liquid. The copper surface in contact with the working fluid was polished using emery paper #600, corresponding to a roughness R_p of $1.1 \mu\text{m}$. Fig. 2 shows a scheme of the

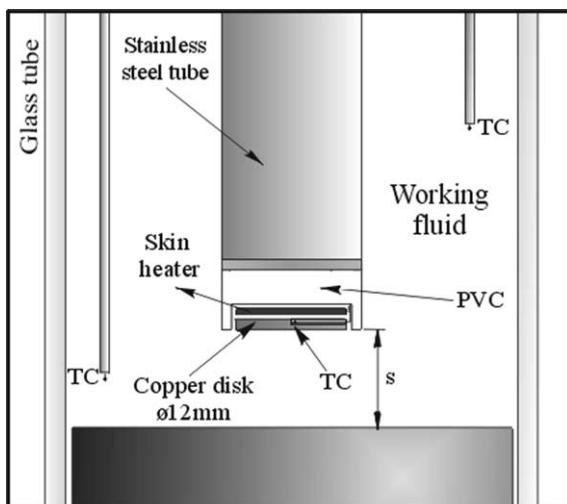


Fig. 2. Test section inside the boiling chamber.

PVC support with the copper disk inside the boiling chamber. The boiling chamber was modified in order to provide the boiling visualization from the bottom, for conditions with a high degree of subcooling in which the liquid bulk temperature was close to 20°C . The PVC support of the test section was beveled to an angle of 45° .

Before each test run the working fluids were heated to very close to the saturation temperature in order to degas them and the liquid and vapor (at the upper part of the boiling chamber) temperatures were monitored. No evidence of significant amounts of gas dissolved in the working liquids was detected on the boiling curves.

A DC power supply, HP6030A, is connected to the skin heater and controlled by a PC using LABVIEW and the previous data acquisition and treatment are carried out by a HP34970A. In the present work the heating mode is by increasing the heat flux. The experimental procedure is programmed in LABVIEW and each test has a 180 s duration for each imposed heat flux followed by an interval of 300 s with the power supply turned-off. Only the temperature data for the last 90 s of the test interval were acquired at a rate of 3 points/s. Different heating procedures were tested: with continuous power increments or with a delay while the power supply was turned-off. The latter was adopted in order to obtain the steady-state condition even with natural convection but the comparison with correlations for one-phase provided by Incropera and DeWitt (1990) did not show good agreement. Using this procedure we could guarantee the steady state condition, even under subcooled conditions and one-phase convection, and this was verified by the temperature history of the copper disk and the fluid. In the literature we can find a great number of studies, such as in Fujita et al. (1988), in which the boiling curves were obtained by decreasing the heat flux. In the present study, because of the low heat flux region of the boiling curve, we decided to employ an experimental procedure with a reduced test duration. The penalty associated with this procedure is the very long time necessary to obtain each average point of the partial boiling curve presented in this study. For a high heat flux region of the boiling curve the steady state condition is easier to obtain.

The temperature uncertainty is $\pm 0.6^\circ\text{C}$, using the same procedure reported by Passos and Reinaldo (2000). The experimental uncertainty for the heat flux is 1%, and those for the heat transfer coefficients vary from 3% to 7% and were computed following the procedure presented by Holman (1989) and Kline (1985).

Due to the great sensitivity of boiling experiments with non-stationary test conditions and also with the experimental procedure, tests were carried out on different days for the same test conditions. Fig. 3 shows an example of this. The data present a good repeatability of the results for two distinct conditions: confined and

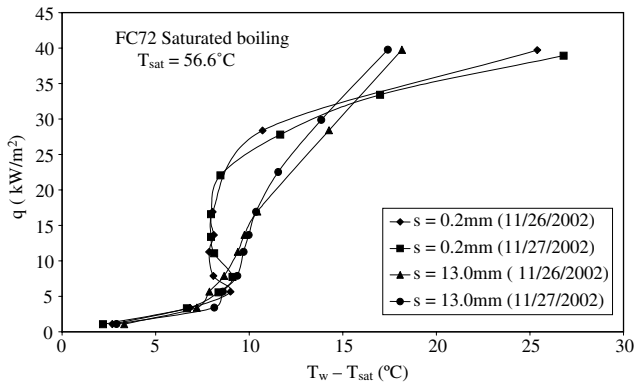


Fig. 3. Boiling curves on different days.

unconfined boiling. In the following figures the indicated bulk temperature, T_{bulk} , represents the average temperature measured using the two thermocouples immersed in the liquid region. For the saturated conditions the nominal T_{sat} is the value furnished by 3M because the bath temperature was controlled to maintain the working fluid very slightly under the saturation temperature, at atmospheric pressure.

3. Results

3.1. Saturated boiling

Fig. 4 shows the effect of the confinement on the partial boiling curve, at saturation temperature, for FC72, for $s = 0.2, 0.5, 1.0$ and 13 mm. The capillary length, Eq. (1), is near 0.8 mm. For these values of s , the Bond number ($= s/L$) is equal to $0.25, 0.63, 1.25$ and 16.25 , respectively. We can observe that except for the case with $s = 13$ mm, the others show a particular dependence on the heat transfer coefficient (or ΔT) of s and q . For $s = 0.2$ and 0.5 and heat flux between 5 and 22 kW/m² ΔT is smaller than that for $s = 13$ mm, for the same heat flux, showing an enhancement of the boiling.

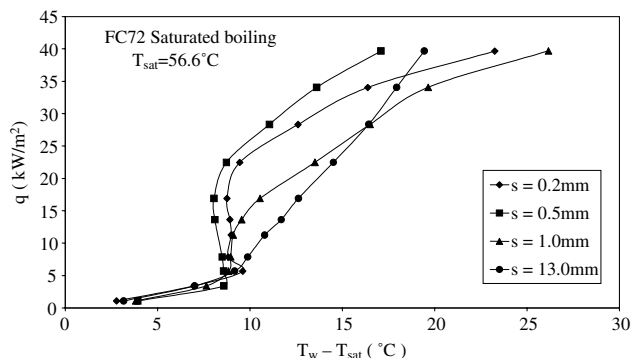


Fig. 4. Confinement effect for FC72.

According to the interpretation of Ishibashi and Nishikawa (1969) and Katto et al. (1977) this effect is due to the evaporation of the liquid film between the flattened bubble and the heating wall. In fact the deformation of the bubbles increases the area of the liquid film and then the increase of vapour mass created in the boiling process allows the efficient heat transfer from the wall to the liquid. For heat flux higher than 22 kW/m² the increase in the ΔT indicates a reduction in the enhancement effect, this being more important for $s = 0.2$ mm, compared with $s = 0.5$ mm. This trend is qualitatively coherent with results presented by Katto et al. (1977) concerning the dryout heat flux and considered in the introduction of this paper. The results of $s = 1$ mm tend to the unconfined case but for heat flux higher than 30 kW/m² the reduction in the heat transfer is more important than for the cases with $s = 0.2$ and 0.5 mm. For $s = 1$ mm the Bond number is close to unity and a confinement with deformation or squeezing of the bubbles is not evident. However, the residence time of the bubbles in the narrow space should be increased because it is more difficult for them to escape to the liquid pool. Fig. 4 shows that for the cases with confinement ($s = 0.2$ and 0.5 mm) the enhancement of the boiling for low heat flux is followed by an increase in the wall temperature for heat fluxes above 25 kW/m². This disappearance of the enhancement effect indicates that these higher values are close to the dryout heat flux. These opposite behaviours agree with the literature as indicated in the introduction and represent the main point to be considered in device and system designs for particular applications.

Fig. 5 shows the heat transfer coefficient, $h = q(T_w - T_{\text{sat}})^{-1}$, against the heat flux for saturated FC72 and the expected results for h using the well known Rohsenow correlations with $C_{\text{sf}} = 0.0054$ and a mean deviation of 15% . The C_{sf} value indicated above is very close to the value for the best fit for the experimental data reported by Geisler and Bar-Cohen (2003). For the cases with confinement we can observe a decrease in h when q is higher than 22 kW/m².

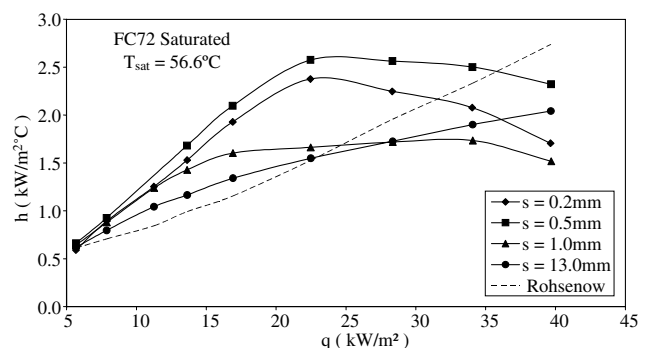


Fig. 5. Heat transfer coefficient against heat flux.

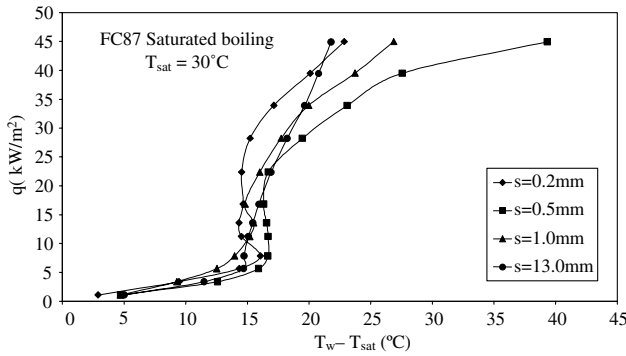


Fig. 6. Confinement effect for FC87.

Fig. 6 shows the FC87 results for different values of s . As in the cases shown in Fig. 4, the effect of confinement is observed for $s = 0.2, 0.5$ and 1 mm. As expected the points corresponding to $s = 2$ mm ($Bo = 2.7$) and $s = 13$ mm are very close and don't present the characteristics of confined boiling. The boiling curves for $s = 0.2$ and 1 mm are similar to those discussed above for the corresponding cases in Fig. 4. For $s = 0.5$ mm, however, the expected enhancement of the boiling under low heat flux was not observed in this work.

3.2. Subcooled boiling

Fig. 7 shows the effect of the bulk temperature for $s = 0.2$ mm. For a bulk temperature of 10 °C an abrupt decrease in the wall temperature after nucleation, close to 22 kW/m² is shown. This was not detected for $T_{bulk} = 30$ °C. Unlike the corresponding case in Fig. 3, for $s = 0.2$ mm, no decrease in the heat transfer for moderate heat flux at 40 kW/m² was obtained in Fig. 7. Since under subcooled conditions, at the same heat flux, the boundary layer thickness is smaller than at saturated boiling the bubbles are also smaller and the results are similar to those without confinement. The small differences in ΔT , less than 4 °C, compared to the bulk temperature difference of 20 °C, confirm the results of Passos and Reinaldo (2000), also observed in Carey

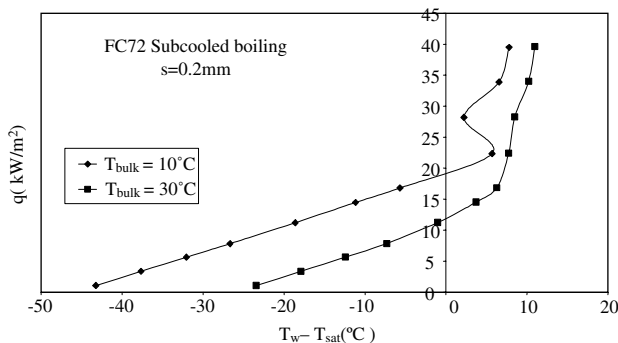


Fig. 7. Effect of the bulk temperature.

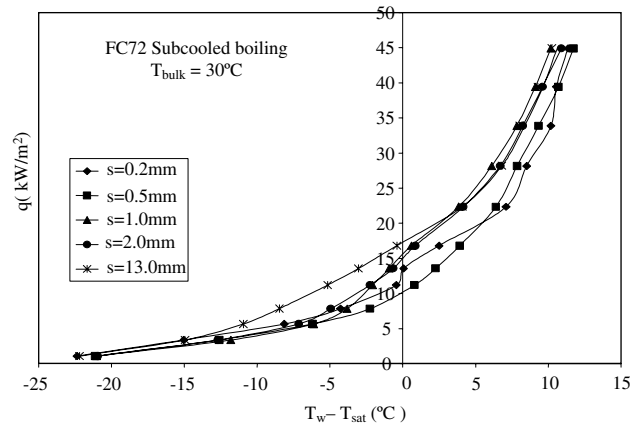


Fig. 8. Confinement effect for FC72.

(1992), showing a slight dependence of the subcooled boiling on the bulk temperature.

Fig. 8 shows the confinement effect for FC72 at a bulk temperature of 30 °C, corresponding to a subcooling degree of 26.6 °C. In the region of single-phase natural convection, particularly for heat flux between 5 and 15 kW/m² the decrease in s , in general, promotes an increase in the wall temperature. The same trend occurs in the subcooled boiling region, above 20 kW/m². Unlike for saturated boiling, see Fig. 4, the confinement increase pushes the curves to the right which indicates a reduction in the heat transfer coefficient. This confinement effect is more evident when we compare the cases with $s \geq 1$ mm with the cases $s = 0.2$ and 0.5 mm. In fact, the modification in the natural convection flows, caused by the more confined conditions, leads to an increase in the liquid temperature in the control volume between the disk and the base of the boiling chamber which plays a similar role in the cases in Fig. 7. This heating of the liquid also depends on the geometric factor.

3.3. Visualization

Fig. 9 shows a sequence of pictures taken from the bottom of the boiling chamber as a function of the distance s and the heat flux. The FC72 is subcooled, close to 20 °C. In all cases an increase in heat flux causes an increase in bubble density and when the s value is small the coalescence of vapor bubbles on the disk. It is interesting to observe the difference between the views for $s = 1$ and 13 mm and those for $s = 0.2$ and 0.5 mm. For $s = 0.2$ and 0.5 mm there is the coexistence of isolated and coalesced bubbles with an increase in bubble density with an increase in heat flux. The co-existence of isolated and large deformed vapor bubbles can explain the relative good thermal performance for the subcooled boiling up to a heat flux of 40 kW/m², as is shown in Figs. 7 and 8. For $s = 1$ and 13 mm the liquid vapor interface is characterized by isolated bubbles but for the more confined case the bubbles are bigger.

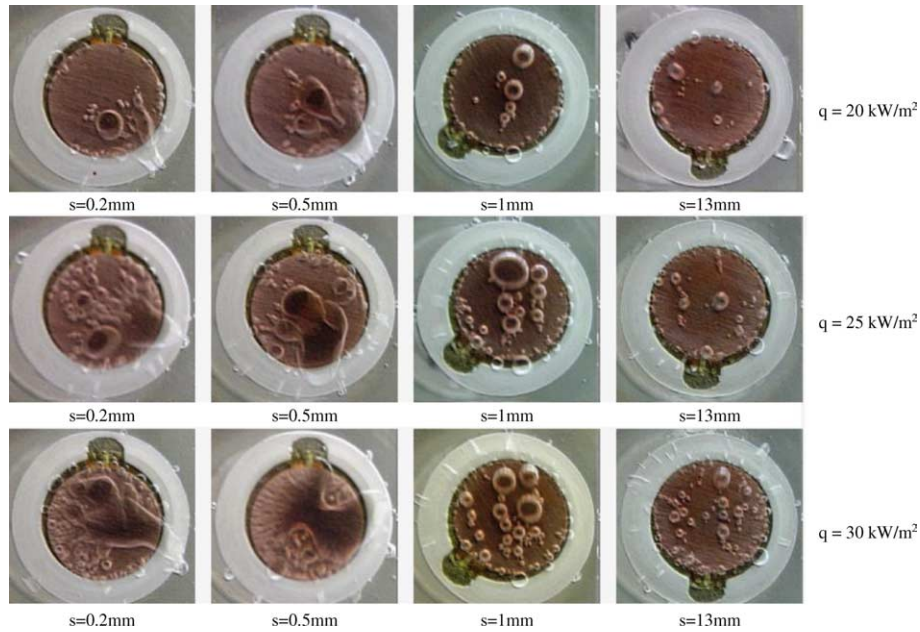


Fig. 9. Visualizations of subcooled boiling as a function of heat flux and s .

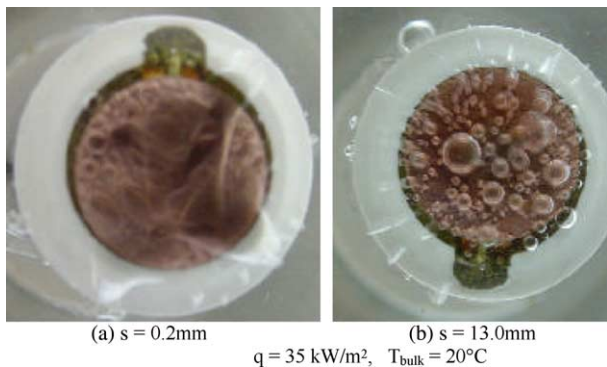


Fig. 10. Subcooling boiling for (a) $s = 0.2$ mm and (b) $s = 13$ mm.

Fig. 10 shows the boiling for the minimum and maximum distances, for a heat flux of 35 kW/m^2 . For $s = 0.2$ mm the coexistence of isolated and coalesced bubbles can explain the efficient heat transfer mechanisms even for this relatively high heat flux. Due to the high degree of subcooling ($= 36.6 \text{ }^\circ\text{C}$) the bubbles are smaller and even for the small distance s the boiling is not confined enough. For saturated boiling with $s = 0.2$ mm, the dryout started close to 22 kW/m^2 .

Modifications in the experimental setup will allow the visualization of boiling for saturated conditions.

4. Discussion

Our results for FC72 and FC87, regarding Figs. 4 and 6, are qualitatively similar and for the cases of $s = 0.2$

and 0.5 mm, in the heat flux range of $7\text{--}22 \text{ kW/m}^2$, the points for FC72 are shifted to the left of $\Delta T = 5\text{--}7 \text{ }^\circ\text{C}$ with respect to FC87.

A comparison of the above results with those published is not an easy task because of the difficulties in finding the same configuration we have. For the unconfined case we took an experimental point from Chang and You (1996) for saturated FC72 on the heated downward facing surface. At 15 kW/m^2 , these authors obtained $\Delta T = 14 \text{ }^\circ\text{C}$, corresponding to a heat transfer coefficient of $1075 \text{ W/m}^2 \text{ K}$. From Fig. 4, for the same heat flux, we obtain $1308 \text{ W/m}^2 \text{ K}$ for the heat transfer coefficient. The ratio of the side length of the heating plate to that of the support of the heating plate can be considered as a second type of confinement. In fact this geometric factor can give an insight into this kind of confinement even for higher Bond numbers. In the study by Chang and You (1996) the ratio is $10/40 = 0.25$ whereas in our case it is $12/20 = 0.6$ which can explain the difference of $+17\%$ in the heat transfer coefficient we have obtained. Chang and You (1996) give the value of 16 kW/m^2 for the critical heat flux which is much lower than the highest heat flux of 40 kW/m^2 in our tests, although in our case the CHF or DHF were not measured. These differences could also be due to the differences in the geometric factors. It is interesting to reinforce that both experimental procedures used a heat flux increase.

Although the boiling visualization was carried out only for subcooling conditions the views in Figs. 9 and 10 show the existence of different mechanisms for small and large Bond numbers and we can expect, for $s = 0.2$

and 0.5 mm, that the CHF is not so far from the maximum heat flux in this study.

The comparison of our results for unconfined boiling with some well known correlations such as those of Cooper (1984) and Stephan and Abdelsalam (1980) shows great differences between them. However, for FC72 the experimental data are very close to those computed using the Rohsenow's correlation with $C_{sf} = 0.0054$, which is very close to the value ($C_{sf} = 0.0055$) obtained by Geisler and Bar-Cohen (2003).

5. Conclusions

In this paper new experimental results from research into confined and unconfined saturated and subcooled FC72 and FC87 boiling heat transfer are presented. The confinement is characterized by the distance between a horizontal downward facing heated plate mounted in parallel with a horizontal unheated wall varying between 0.2 and 13 mm. The main results are the following:

- (i) For saturated boiling a decrease in the distance between the plates increases the heat transfer coefficient for almost the entire range (5–35 kW/m²). Above 22 kW/m² for the confined conditions of 0.2 and 0.5 mm the wall temperature increases. Even for the case with the Bond number 1.25, for which the heat transfer mechanisms may be considered not so different to those of the unconfined case, the heat transfer coefficient may be also influenced by the geometric factor that characterises the particular test section geometry and which may result in the bubbles being retained longer inside. For both fluids, for $s = 0.2$ and 0.5 mm, the increase in the wall temperature for heat fluxes above 22 kW/m² shows a reduction in the maximum heat flux when s decreases.
- (ii) For subcooled conditions the effect of the confinement is the opposite to that for saturated boiling and an increase in the confinement causes a reduction in the heat transfer coefficient. There is a slight dependence of the subcooling degree on the heat transfer coefficient.
- (iii) The visualization for subcooled boiling shows the coexistence of isolated and large coalesced deformed bubbles on the copper disk for $s = 0.2$ and 0.5 mm whereas for $s = 1$ and 13 mm the two-phase configuration is characterized by isolated bubbles with some larger spherical bubbles in the case of $s = 1$ mm.

Acknowledgements

The authors are grateful for the support of the Brazilian Space Agency (AEB), CAPES and the Research Council of Brazil (CNPq) in performing this study. The authors extend their thanks to Mr. R. Van San from 3M Corporation for supplying the fluids.

References

- Arlabosse, P., Tadrist, H., Faure, R., Pantaloni, J., Tadrist, L., 1998. Contribution à l'analyse de l'ébullition nucléée: étude expérimentale de la convection thermocapillaire autour d'une bulle. *Entropie* 215, 64–68.
- Bonjour, J., Lallemand, M., 1997. Effects of confinement and pressure on critical heat flux during natural convective boiling in vertical channels. *Int. Commun. Heat Mass Transfer* 24 (2), 191–200.
- Carey, V.P., 1992. *Liquid-Vapor Phase-Change Phenomena*. Hemisphere/Taylor & Francis, Washington, DC.
- Chang, J.Y., You, S.M., 1996. Heater orientation effects on pool boiling of micro-porous-enhanced surfaces in saturated FC-72. *J. Heat Transfer-Trans. ASME* 118, 937–943.
- Cooper, M.G., 1984. Saturation nucleate pool boiling: a simple correlation. 1st UK National Conference on Heat Transfer, vol. 2, pp. 785–793 (I. Chemical E. Symposium Series no. 86).
- Fujita, Y., Ohta, H., Uchida, S., Nishikawa, K., 1988. Nucleate boiling heat transfer and critical heat flux in narrow space between rectangular surfaces. *Int. J. Heat Mass Transfer* 31, 229–239.
- Geisler, K.J.L., Bar-Cohen, A., 2003. Nucleate pool boiling heat transfer in narrow vertical channels. In: *Proceedings of the International Conference on Boiling Heat transfer. Session XII, Montego Bay, Jamaica, University of Florida*, 5 p.
- Holman, J.P., 1989. *Experimental Methods for Engineers*. McGraw-Hill, New York.
- Incropera, F.P., DeWitt, D.P., 1990. *Introduction to Heat Transfer*, third ed. John Wiley & Sons, New York. pp. 460–465.
- Ishibashi, E., Nishikawa, K., 1969. Saturated boiling heat transfer in narrow spaces. *Int. J. Heat Mass Transfer* 12, 863–894.
- Katto, Y., Yokoya, S., Teraoka, K., 1977. Nucleate and transition boiling in a narrow space between two horizontal, parallel disk surfaces. *Bull. JSME* 20 (143), 638–643.
- Kline, S.J., 1985. The purposes of uncertainty analysis. *ASME J. Fluid Mech.* 107, 153–160.
- Nishikawa, K., Fujita, Y., Uchida, S., Ohta, H., 1984. Effect of surface configuration on nucleate boiling heat transfer. *Int. J. Heat Mass Transfer* 27, 1559–1571.
- Passos, J.C., Reinaldo, R.F., 2000. Analysis of pool boiling within smooth and grooved tubes. *ETFS-Exp. Therm. Fluid Sci.* 22, 35–44.
- Passos, J.C., Misale, M., Lallemand, M., 2002. Some considerations regarding the enhancement of nucleate pool boiling. 9th Brazilian Congress of Thermal Engineering and Sciences. ABCM/CD-ROM, pp. 1–11.
- Stephan, K., Abdelsalam, M., 1980. Heat transfer correlations for natural convection boiling. *Int. J. Heat Mass Transfer* 23, 73–87.
- Straub, J., Zell, M., Voel, B., 1990. Pool boiling in a reduced gravity field. In: *Proceedings of The Ninth International Heat Transfer Conference, Jerusalem*, pp. 91–112.
- Yao, S.C., Chang, Y., 1983. Pool boiling heat transfer in a confined space. *Int. J. Heat Mass Transfer* 26 (6), 841–848.